galaxies

MDPI

Article

Applications of the Irbene Single-Baseline Radio Interferometer

Ivar Shmeld [1], Vladislavs Bezrukovs [1,*], Jānis Šteinbergs [1], Karina Šķirmante [1], Artis Aberfelds [1], Sergey A. Belov [2], Ross A. Burns [1,3], Dmitrii Y. Kolotkov [1,2], Valery M. Nakariakov [1,2], Dmitrijs Bezrukovs [1], Matīss Purviņš [1], Aija Kalniņa [1], Arturs Orbidans [1], Marcis Bleiders [1] and Marina Konuhova [1,4,*]

[1] Engineering Research Institute "Ventspils International Radio Astronomy Centre (VIRAC)", Ventspils University of Applied Sciences, Inzenieru 101, LV-3601 Ventspils, Latvia; ivarss@venta.lv (I.S.); janis.steinbergs@venta.lv (J.Š.); karina.skirmante@venta.lv (K.Š.); artis.aberfelds@venta.lv (A.A.); ross.burns@riken.jp (R.A.B.); d.kolotkov.1@warwick.ac.uk (D.Y.K.); v.nakariakov@warwick.ac.uk (V.M.N.); dmitrijs.bezrukovs@venta.lv (D.B.); s22purvmati@venta.lv (M.P.); aija.kalnina@venta.lv (A.K.); arturs.orbidans@venta.lv (A.O.); marcis.bleiders@venta.lv (M.B.)

[2] Centre for Fusion, Space and Astrophysics, Department of Physics, University of Warwick, Coventry CV4 7AL, UK; sergey.belov@warwick.ac.uk

[3] RIKEN Pioneering Research Institute, 2-1 Hirosawa, Wako-shi 351-0198, Saitama, Japan

[4] Institute of Solid State Physics, University of Latvia, 8 Kengaraga, LV-1063 Riga, Latvia

* Correspondence: vladislavsb@venta.lv (V.B.); marina.konuhova@cfi.lu.lv (M.K.)

Abstract

The Irbene single-baseline radio interferometer (ISBI), operated by the Ventspils International Radio Astronomy Centre (VIRAC), offers a rare and versatile configuration in modern radio astronomy. Combining the 32-m and 16-m fully steerable parabolic radio telescopes separated by an 800-m baseline, this system possesses a unique capability for high-sensitivity, time-domain interferometric observations. Unlike large interferometric arrays optimized for sub-arcsecond resolution imaging, the Irbene system is tailored for studies that require high temporal resolution and a strong signal-to-noise ratio. This paper reviews key scientific applications of the Irbene interferometer, including simultaneous methanol maser and radio continuum variability studies, high-cadence monitoring of quasi-periodic pulsations (QPPs) in stellar flares, ionospheric diagnostics using GNSS signals, orbit determination of navigation satellites and forward scatter radar techniques for space object detection. These diverse applications demonstrate the scientific potential of compact interferometric systems in an era dominated by large-scale observatories.

Keywords: radio interferometry; single-baseline interferometer; Irbene observatory; GNSS VLBI; ionospheric remote sensing; methanol masers; QPPs; stellar flares; space situational awareness; forward scatter radar

Academic Editor: Wenwu Tian

Received: 17 June 2025
Revised: 18 September 2025
Accepted: 16 October 2025
Published: 3 November 2025

Citation: Shmeld, I.; Bezrukovs, V.; Šteinbergs, J.; Šķirmante, K.; Aberfelds, A.; Belov, S.A.; Burns, R.A.; Kolotkov, D.Y.; Nakariakov, V.M.; Bezrukovs, D.; et al. Applications of the Irbene Single-Baseline Radio Interferometer. *Galaxies* **2025**, *13*, 126. https://doi.org/10.3390/galaxies13060126

1. Introduction

Astrophysical research using radio interferometry began in 1946, when the first successful experiments demonstrated that a pair of radio antennas could achieve angular resolutions far beyond those possible with single-dish telescopes at the time [1]. This breakthrough laid the foundation for a new era in radio astronomy. By the 1960s, interferometry had become the dominant observational technique, enabling astronomers to resolve compact structures across vast cosmic distances. Today, large-scale interferometric arrays such as the European VLBI Network (EVN), the Very Long Baseline Array (VLBA), and the Atacama Large Millimeter/submillimeter Array (ALMA) remain at the forefront of high-resolution radio astronomy [2–4].

A landmark achievement in this field was delivered by the Event Horizon Telescope (EHT), which, through global VLBI at millimetre wavelengths, produced the first image of the black hole shadow in M87 and later imaged Sagittarius A*, the supermassive black hole at the centre of the Milky Way [5,6]. Building upon this foundation, the next-generation Event Horizon Telescope (ngEHT) aims to extend the array with additional stations and advanced instrumentation, enabling dynamic imaging and polarimetric studies at horizon scales [7]. In the southern hemisphere, the MeerKAT interferometer has become a cornerstone facility, contributing to deep continuum mapping, pulsar timing, and large-scale surveys of cosmic structures [8]. Similarly, the Australian Square Kilometre Array Pathfinder (ASKAP) has pioneered wide-field radio surveys and played a leading role in the discovery and localization of Fast Radio Bursts [9]. Together, these facilities exemplify the global scope of contemporary radio interferometry and the complementary strategies adopted to address diverse astrophysical challenges.

In parallel, the development of large single-dish telescopes has pushed the boundaries of sensitivity and backend processing capabilities. The 100-m Effelsberg Radio Telescope in Germany [10] and the Five-hundred-meter Aperture Spherical Telescope (FAST) in China [11] are among the most sensitive radio observatories in the world. These instruments are particularly valuable for studies requiring broad frequency coverage, high time resolution, and the detection of faint signals. However, only a few of these great facilities are available and in high demand, making regular access difficult for projects that rely on continuous or high-cadence observations.

In contrast, short-baseline interferometers—typically composed of just two or a few antennas—offer a practical alternative when sub-milliarcsecond spatial resolution is not required. Although they lack the extreme resolving power of Very Long Baseline Interferometry (VLBI) systems, they provide excellent sensitivity and robust signal-to-noise ratios and can generally provide flexible time allocation. These features make them well suited for high-cadence monitoring of variable astrophysical phenomena such as maser flares, stellar outbursts, and ionospheric disturbances [12–14].

Historically, one of the most influential compact arrays was the Westerbork Synthesis Radio Telescope (WSRT), which operated as a 14-element linear interferometer in the Netherlands. For decades, it played a key role in Galactic plane surveys and H I studies before ceasing operations in its classic array mode [15].

Currently, the Karl G. Jansky Very Large Array (VLA) represents the most powerful short-to-intermediate baseline system, combining high sensitivity with wide frequency coverage. However, the VLA is heavily oversubscribed, and its periodic reconfiguration schedule—while scientifically valuable—can limit continuous or time-domain observations of transient events [16].

A distinct advantage of short-baseline arrays is their sensitivity to extended, low-surface-brightness emission that is often resolved out by long-baseline VLBI networks. For instance, compact thermal sources such as ultra-compact H II regions, spanning several arcseconds, are typically undetectable in VLBI due to the absence of short baselines. Observing such structures would require substantial integration time on large single-dish stations or densely filled hybrid arrays—both resource intensive options [17,18].

Next-generation facilities such as the Square Kilometre Array (SKA-mid) and the next-generation VLA (ngVLA) are designed to close the gap between short-baseline arrays and VLBI, combining high angular resolution with enhanced surface brightness sensitivity. Until such systems become fully operational, compact arrays like the Irbene single-baseline interferometer remain strategically important for time-domain radio astronomy and for detecting processes that would otherwise be missed by long-baseline systems [19,20].

Finally, a two-element interferometer can approach the sensitivity of a single telescope with an equivalent combined collecting area. The cross-correlation process suppresses uncorrelated noise while preserving coherent astronomical signals, enabling operation near thermal noise limits. This makes compact interferometers particularly effective for detecting low amplitude flux variations not readily observable with single-dish systems or oversubscribed large arrays [17].

This paper presents the technical configuration and key scientific applications of the Irbene single-baseline radio interferometer, operated by the Ventspils International Radio Astronomy Centre (VIRAC). The system comprises two fully steerable parabolic antennas—RT-32 (32 m) and RT-16 (16 m)—separated by an 800-m baseline, as illustrated in Figure 1. The interferometer is designed for high-sensitivity, high-cadence, and broadband observations. During periods of lower observing demand, it can be effectively utilized for time-domain astrophysics studies, emphasizing temporal coverage over angular resolution.

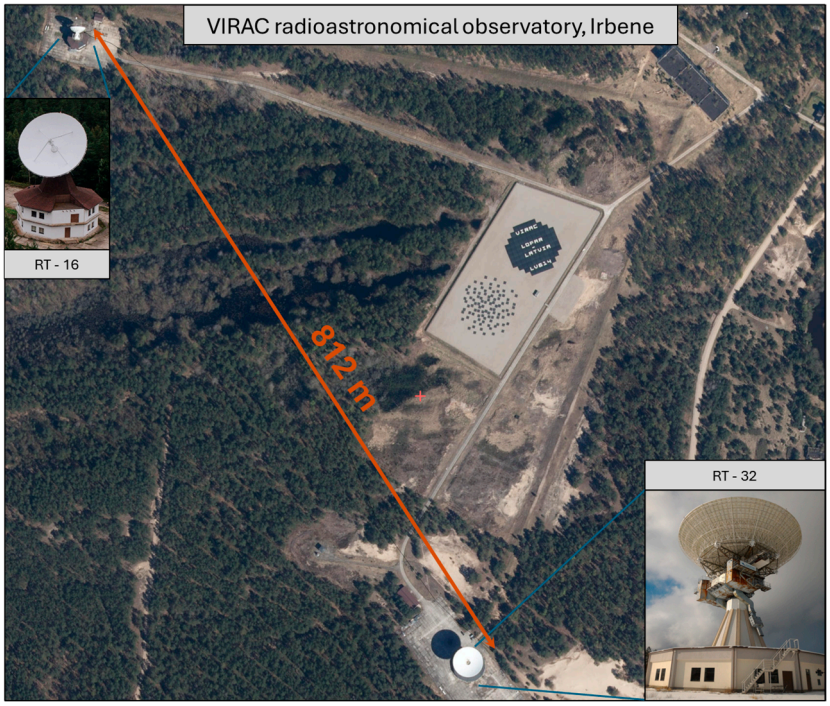

Figure 1. The Irbene single-baseline radio interferometer, operated by the Ventspils International Radio Astronomy Centre (VIRAC). The system comprises two fully steerable parabolic antennas—RT-32 (32 m) and RT-16 (16 m)—separated by an 800-m baseline. Map: The Latvian Geospatial Information Agency.

Applications covered in this paper include:

- Continuum flux variability monitoring in star-forming regions associated with methanol maser sources.
- Observations of quasi-periodic pulsations (QPPs) in stellar flares.
- VLBI-based ionospheric diagnostics and GNSS satellite orbit determination.
- Detection of space objects using forward scatter radar methods.

In a research environment increasingly dominated by large, multi-user observatories, compact interferometric systems like Irbene offer a complementary approach. Their adaptability and autonomy provide valuable access to high-cadence radio observations, fulfilling scientific requirements that would otherwise remain underserved.

2. Interferometric System and Receiver Architecture at the Irbene Observatory

The Irbene Radio Astronomy Observatory, part of the Ventspils International Radio Astronomy Centre (VIRAC) operated by Ventspils University of Applied Sciences (VUAS), has undergone significant technological transformation since 2011. These upgrades have positioned it as a modern radio astronomical facility capable of participating in both national and international Very Long Baseline Interferometry (VLBI) campaigns [21,22]. The observatory operates two fully steerable parabolic radio telescopes—RT-32 and RT-16—with main reflector diameters of 32 m and 16 m, respectively. Separated by 800 m, these antennas form the Irbene single-baseline interferometer.

Following major enhancements to their receiving and backend systems, the RT-32 and RT-16 telescopes have actively participated in international VLBI observations since October 2015, including regular sessions with the European VLBI Network (EVN) and the EVN-Lite array. In addition to supporting a wide range of astrophysical investigations, such as astrometry, planetary radio emission monitoring, ionospheric research, near-Earth object (NEO) tracking, and Fast Radio Burst (FRB) studies [23–26], the Irbene radio telescopes have also contributed to the Radio Astron space VLBI mission, enabling high-resolution observations of AGN, pulsars, and cosmic masers, and yielding unprecedented microarc second-scale imaging and measurements of extreme brightness temperatures [27].

2.1. VLBI Instrumentation and Signal Processing

The Irbene interferometer is equipped with a modern signal acquisition and timing chain, optimized for high-precision geodetic and astronomical VLBI applications. Signal digitization is performed using Digital Baseband Converters (DBBC2), which support two-bit sampling, multiband operation and flexible, programmable spectral line registration backend based on the Ettus "USRP X300" software (https://www.ettus.com/all-products/x300-kit/&quot (accessed on 15 October 2025)) defined radio [28–30].

Each antenna site records digitized data using high-throughput storage systems, including two *FlexBuff* servers with capacities of 288 TB and 64 TB, respectively. For long-term archiving, a 2 PB magnetic tape-based storage system—originally developed for LOFAR data—is also available.

Timing and frequency synchronization are anchored by a *T4 Science Hydrogen Maser 3000*, located at the RT-16 facility. Time and frequency signals are distributed to RT-32 via an optical fiber link using a *White Rabbit* solution, provided and installed by Safran Corporation, Paris, France. This setup achieves synchronization with an Allan variance better than 10^{-15} over a one-day operational period under typical daytime temperature conditions. [31,32].

Data correlation is performed using the Software FX Correlator (SFXC) (version DiFX-2.8.1), developed at the Joint Institute for VLBI in Europe (JIVE) [33]. A typical spectral resolution of 0.01 MHz is used during correlation, yielding a maser line velocity resolution of approximately 0.088 km s^{-1} at 6.7 GHz. Post-correlation data processing is carried out using the Astronomical Image Processing System (AIPS) (version number: 31DEC25) and Common Astronomy Software Applications (CASA) (version number: 6.7). Regarding sensitivity, the interferometer can currently achieve clear detections of 5 cm radio continuum sources with flux densities of less than 100 mJy, as discussed in the following section (Section 3.2). Several factors negatively impacting the sensitivity of the interferometer include a movement of the C-band receiver in the RT-32 from the central focal point to an offset position, in order to accommodate additional receivers, and deterioration of the alignment of surface panels on the RT-32 since the initial antenna refurbishment in 2015, leading to a compromised surface accuracy. The resulting aperture efficiency of the RT-32

is estimated to be 30% at these frequencies. Finally, the ability for the interferometer to maximise signal to noise relies on the integration of signals coherently in the time and frequency domains. This is dependent on the success of the data reduction pipeline in measuring and solving residual delays and phases, both dynamic and systematic, which were not treated in the pre-correlation delay model. To this end, continued optimisation of the data reduction pipeline are ongoing (Burns et al. in prep [34]).

To streamline observation scheduling and minimize operational overhead, a custom-developed observation control system has been implemented. This software supports predefined scripts specifying source positions, frequency configurations, and calibration sequences. These routines are executed autonomously, enabling efficient, frequency-agile operations.

2.2. Broadband 4.5–8.8 GHz Cryogenic Receiver Systems

Both RT-32 and RT-16 telescopes are equipped with broadband cryogenic receiver systems developed and installed by Tecnologías de Telecomunicaciones e Información, TTI, Spain. These receivers (shown on Figure 2) operate over the frequency range of 4.5–8.8 GHz and are optimized for VLBI applications in the C, M and X bands [35,36]. Key technical features include:

- Dual Circular Polarization: Both left and right circular polarization (LCP and RCP) signals are received simultaneously.
- Cryogenically Cooled Front-End: The RF front-end includes a corrugated feed horn, polarizer, orthomode transducer (OMT), and low-noise amplifiers (LNAs) cooled to 14 K. The first stage operates at 46 K, and the polarizer at 20 K using a closed-cycle helium refrigerator.
- Intermediate Frequency (IF) Subsystem: The RF signal is filtered and down converted to an IF band (0.3–1.5 GHz) using a switchable synthesizer and bandpass filters. The IF system exhibits low phase noise and high spectral purity.
- Calibration Infrastructure includes phase calibration tone injection (typically 1 MHz spacing) and broadband noise diode for amplitude calibration.

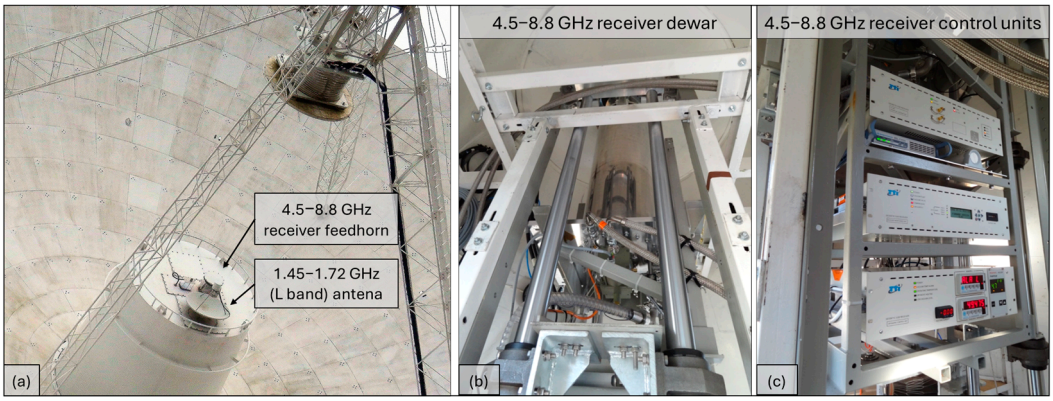

Figure 2. Broadband 4.5–8.8 GHz cryogenic receiver system installed on the RT-32 radio telescope. (**a**) Antenna overview showing the primary and secondary mirrors along with the vertex room; (**b**) Receiver dewar installed inside the vertex room; (**c**) Receiver control units installed in the vertex room beneath the dewar.

Measured system temperatures are approximately 30 K for RT-32 and 35 K for RT-16, yielding system equivalent flux densities (SEFD) between 300–400 Jy, making the Irbene facility comparable in sensitivity to other EVN stations. The cryogenic receivers are used in

both standalone and VLBI interferometric observations, supporting high dynamic range and low-noise requirements [37–39].

As of 2025, the RT-16 radio telescope at the Irbene Observatory is undergoing comprehensive modernization. A key element of this upgrade, scheduled for implementation in Q1 2026, is the installation of a new cryogenically-cooled receiver system designed, in-house, capable of simultaneous dual-band operation in the X (8–12 GHz) and Ka (26.5–40 GHz) frequency ranges. Following this upgrade, single-baseline interferometric observations at Irbene will remain limited to the X band, as the RT-32 telescope is not yet equipped with a Ka-band receiver. However, the planned future integration of a Ka-band receiver on RT-32 will enable expansion of the interferometric system's operational bandwidth, significantly enhancing the scientific potential of the Irbene baseline array.

2.3. L-Band Observation Capability of the RT-32 Telescope

To support scientific observations in the L-band (1.45–1.72 GHz)—particularly for strong radio sources, GNSS satellite tracking, and ionospheric studies—a dedicated front-end system has been developed for the RT-32 telescope [40,41].

A composite feed antenna was built and installed at the RT-32 telescope's secondary focus, with a lateral phase centre offset of 1 m and a tilt angle of 8°. The receiver design employs a three-mirror optical configuration, in which a compact parabolic reflector redirects incoming radiation toward a dual-polarized feed horn antenna, providing an efficient and space-saving solution for L-band observations. As shown in Figure 3, this configuration fits within the RT-32's structural constraints and eliminates the need for mechanical modifications to the telescope's vertex room. Non-cryogenic operation was deliberately chosen to ensure low-maintenance and cost-effective performance. The system provides dual polarization capability, supporting both left-hand and right-hand circular polarizations.

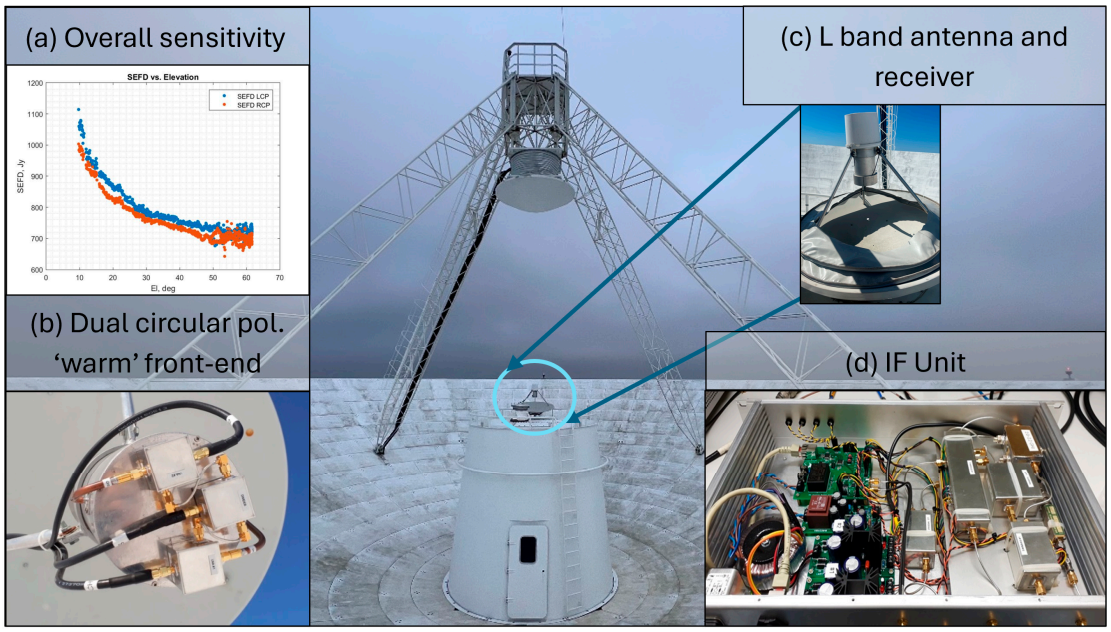

Figure 3. Uncooled L-band receiver with a three-mirror optical system installed on the RT-32 radio telescope. (**a**) Sensitivity plot: system equivalent flux density (SEFD) in Jy versus elevation (degrees); (**b**) Dual circular polarization "warm" front-end view; (**c**) L-band receiver positioned at the antenna focal point; (**d**) Intermediate frequency (IF) unit mounted inside the vertex room.

Performance testing indicates that the L-band system achieves an average SEFD of approximately 750 Jy at 1650 MHz. Despite the absence of cryogenic cooling, this sensitivity is sufficient for several important scientific and applied applications, including:

- GNSS interferometry: Tracking GPS, Galileo, and similar satellite systems for orbit determination and ionospheric scintillation studies.
- Spectral line observations: Detection of weak spectral lines, such as hydroxyl (OH) masers [42].
- VLBI observations of GNSS satellites: Enabling joint VLBI–SLR (Satellite Laser Ranging) campaigns that combine angular and ranging measurements.
- Participation in global VLBI campaigns: Despite its relatively modest sensitivity, the L-band receiver has demonstrated reliable performance in international VLBI sessions, particularly within the EVN network.

The availability of this L-band system significantly enhances the frequency agility and scientific versatility of the RT-32 telescope, particularly for space weather research and near-Earth ionospheric diagnostics in multi-frequency VLBI experiments.

3. Science Applications of the Irbene Interferometer

3.1. Irbene Interferometer for Orbit Determination and Ionospheric Studies

VIRAC has expanded its scientific program to include L-band interferometric observations for both atmospheric and space-based research. The centre's infrastructure—particularly the RT-32 and RT-16 radio telescopes—plays a key role in studying ionospheric dynamics and in the precise determination of satellite orbits using signals from Global Navigation Satellite Systems (GNSS).

3.1.1. Ionospheric Remote Sensing Using GNSS Signals

Since 2012, VIRAC has participated in joint VLBI campaigns with Pan-Eurasian partners [21], including experiments focused on remote sensing of the ionosphere using navigation satellites such as GPS, Galileo, and GLONASS as coherent, high-power signal sources. These satellites emit well-characterized L-band signals (~1.6 GHz), making them ideal for probing ionospheric conditions with high temporal and spatial resolution [43]. In a series of experiments, the ionosphere was deliberately excited using the Sura Ionospheric Heating Facility[1] located near Vasilsursk, operated by the Radio physical Research Institute (NIRFI) in Nizhny Novgorod. As of September 2020, NIRFI has been integrated into Lobachevsky University, becoming one of its research divisions. These experiments resulted in significant variations in GNSS signal amplitude and spectral structure, effects directly attributable to electron density fluctuations [44,45].

For these experiments, the RT-16 antenna was then equipped with a dedicated L-band feed featuring spiral antennas optimized for right-hand circular polarization, ensuring efficient GNSS signal reception. Interferometric observations were conducted in coordination with the Irbene radio telescopes and partner antennas in Nizhny Novgorod. As illustrated in Figure 4, these included RT-2—a 2 m antenna located on the roof of Lobachevsky State University of Nizhny Novgorod—and St. Pustyn RT-14, a 14 m radio telescope located at the Staraya Pustyn site. This configuration enabled simultaneous investigation of both natural and artificially induced ionospheric disturbances.

These experiments confirmed the high sensitivity of VLBI techniques to electron density irregularities, enabling the estimation of key ionospheric parameters such as spatial spectral indices, irregularity drift velocities, and anisotropies. The VLBI system at Irbene thus serves as a powerful remote sensing tool for characterizing both naturally occurring and artificially induced ionospheric phenomena.

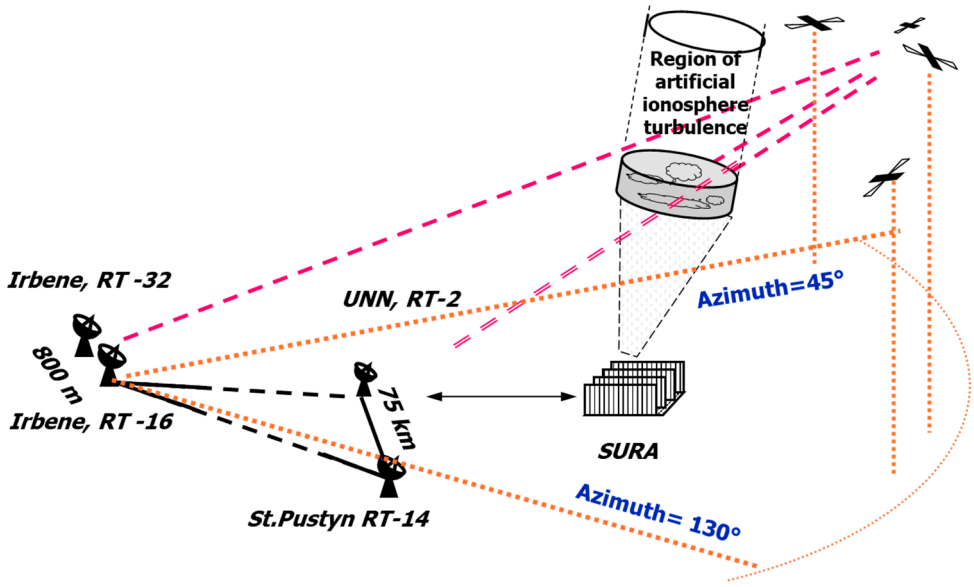

Figure 4. Diagram of ionospheric disturbance probing during a heating experiment using the SURA ionospheric facility. GNSS signal detection is carried out by a distributed antenna network operating in both interferometric and single-station modes.

3.1.2. Interferometric Satellite Orbit Determination

Building on its capabilities in ionospheric sensing, VIRAC has conducted several campaigns focused on applying radio interferometric methods for GNSS satellite orbit determination. In 2016 and 2017, VIRAC collaborated with the Institute of Astronomy of the University of Latvia (SLR station Riga) and other observatories [40] to perform simultaneous radio interferometric and Satellite Laser Ranging (SLR) observations of GNSS satellites equipped with laser retroreflectors. This dual-technology approach aimed to combine the high angular precision of VLBI with the sub-centimetre range accuracy of SLR, thereby enhancing the accuracy and robustness of satellite orbit solutions [46].

For example, during the NKA41 (23 September 2017) and NKA42 (24 September 2017) observation campaigns, the RT-32 and RT-16 radio telescopes tracked more than 25 GPS and GLONASS satellites using L-band receivers. Observations were coordinated with the Riga SLR station and focused on satellites with retroreflectors, including GLONASS-116, -131, -136, and Galileo-206. Calibration sources *3C 123* and *Cas A* (Cassiopeia A) were included to validate system performance.

VLBI data were recorded in VDIF format using FlexBuff systems at RT-32 and Mark 5 systems at RT-16. (Note: the Mark 5 system at RT-16 has since been replaced with a newer FlexBuff server). Observations were conducted with an 8 MHz bandwidth and left-hand circular polarization. Data correlation and processing were carried out using the "KANA" software correlator developed at VIRAC [47] This in-house tool, currently in an alpha stage of development, supports a wide range of data formats and generates time-resolved interferometric outputs suitable for orbit analysis.

Simultaneously, SLR measurements provided highly accurate range data, with RMS residuals as low as ~25 picoseconds. These data enabled cross-validation with VLBI-derived angular measurements. Overlapping VLBI–SLR observation windows allowed for synchronized acquisition, which is critical for producing hybrid orbit solutions and refining GNSS satellite orbital parameters [46,48].

These multidisciplinary, dual-technology campaigns demonstrated the scientific feasibility and utility of integrating VLBI with other space geodetic techniques. VLBI contributes precise angular and angular velocity measurements, while SLR supplies abso-

lute range information—together enabling full six-parameter orbit reconstruction under appropriate conditions.

Potential applications of such integrated observation strategies include:

- Real-time orbit monitoring and anomaly detection (e.g., post-collision analysis).
- Augmentation of GNSS ephemeris data and alignment of terrestrial and celestial reference frames.
- Calibration and validation of ionospheric delay models used in satellite navigation.
- Maintenance of Earth-space coordinate systems through combined VLBI–SLR referencing.

The demonstrated capabilities of the Irbene facility in both atmospheric diagnostics and precision satellite tracking underscore its strategic role in space geodesy, space situational awareness, and the broader scientific investigation of near-Earth space environments.

3.1.3. Application of Forward Scatter Radar Method in Space Object Detection

A complementary experimental approach to space object detection is the use of the Forward Scatter Radar (FSR) method, which relies on the natural emission of powerful extraterrestrial radio sources (e.g., the Sun or Cassiopeia A) or signals from spacecraft transmitters as probing radiation (see Figure 5).

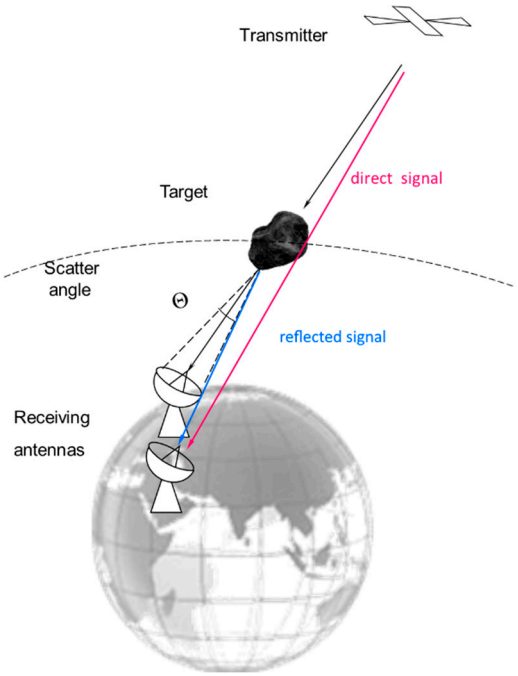

Figure 5. Diagram of the Forward Scatter Radar (FSR) observational experiment using the RT-32 and RT-16 telescopes at Irbene. GNSS satellites and natural radio sources serve as transmitters, while reflections from aircraft and space debris are detected via bistatic and interferometric configurations.

Unlike traditional monostatic radar systems, the FSR method utilizes bistatic radar configurations, significantly increasing detection probabilities by exploiting the forward scatter effect. This effect is characterized by enhanced scattering in the direction of the transmitter, largely independent of the object's shape and material. At VIRAC, the FSR method has been validated through a series of successful experiments using both single-dish and single-baseline interferometer configurations. The RT-32 and RT-16 telescopes at Irbene were used to track reflections of GNSS signals (e.g., GPS, Galileo) from aircraft and space debris objects [49].

The methodology included automated identification of suitable observation opportunities by matching visible GNSS satellites with aircraft or space debris positions within the

antenna's line of sight. Observations showed distinct reflection patterns consistent with theoretical forward scatter predictions.

Validation experiments were carried out at VIRAC using the RT-32 and RT-16 telescopes in both single-dish and interferometric modes, with GNSS (GPS, Galileo, GLONASS, BeiDou) signals serving as probing radiation. Targets included aircrafts, the International Space Station, and large debris fragments in high orbits. Distinct reflection patterns were detected that coincided with predicted flyby times, confirming the feasibility of the method. An example of the results is shown Figure 6 presents a typical result of data processing for the flyby of a space debris fragment at a small angular distance from the "transmitter–receiver" baseline (about 50 arcmin). The interferometer output is shown in the "amplitude–frequency–time" plane for a 30 s interval. Two responses are clearly visible: one from a slowly moving GNSS satellite, which maintains an almost constant frequency due to compensation of frequency and delay shifts during processing, and another from a fast-moving object, exhibiting an interference frequency that varies linearly with time. Successful correlations were achieved in more than half of the observation attempts, demonstrating that the system can separate reflected/scattered signals from direct transmissions and provide reliable detections of moving objects.

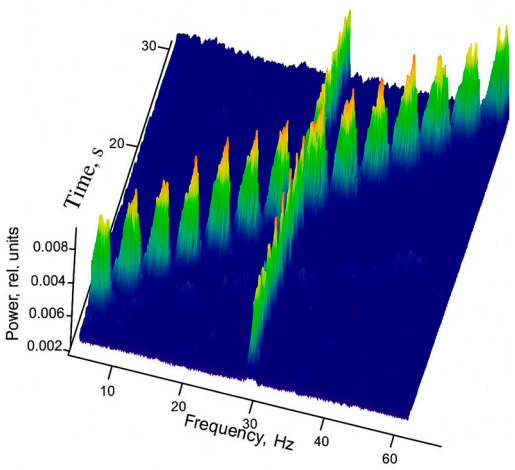

Figure 6. Spectral response of the RT-32–RT-16 interferometer during the flyby of space debris fragment No. 16182 near the "GPS PRN05 transmitter—Irbene interferometer" line of sight (18 March 2021, 17:11:01 UTC). The interferometer output over a 30 s interval shows two signals: a nearly constant-frequency trace from the GNSS satellite (reference source) and a drifting interference pattern from the fast-moving debris. The coincidence of the drifting signal with the predicted flyby time confirms the detection of the object using the forward scatter radar (FSR) method.

Further development is underway to enhance sensitivity and applicability of the method, including the integration of LOFAR (Low-Frequency Array) technology at VIRAC. LOFAR's wider beams and higher sensitivity promise improved performance in detecting weak scattered signals from near-Earth objects and enhancing ionospheric fluctuation monitoring capabilities for better positioning accuracy.

The FSR method, especially when combined with interferometric and LOFAR techniques, provides a valuable addition to the toolkit of planetary defence and space situational awareness systems.

3.2. Single-Baseline Radio Interferometer for OH and Methanol Maser Observations in the Era of Transient Astrophysics

Since 2017, VIRAC has conducted a long-term single dish monitoring program focused on the variability of 6.7 GHz Class II methanol masers—key tracers of high-mass star formation. Using the RT-32 and RT-16 radio telescopes, the program observed 42 maser sources

between March 2017 and October 2022. Observations were typically performed every 5–7 days, with increased cadence for sources exhibiting notable variability. Approximately 95% of the measurements were conducted using RT-16.

The campaign revealed significant variability in more than 55% of the sources, encompassing low-amplitude, periodic, irregular, synchronized, and anti-correlated behaviours among spectral components. These findings underscore the dynamic nature of maser emission and its sensitivity to evolving physical conditions within protostellar environments [50–53].

To enhance its observational capabilities, VIRAC deployed a single-baseline interferometer operating at 6.7 GHz, combining the RT-32 and RT-16 telescopes, which are separated by 800 m. This configuration provides an angular resolution of approximately 15 arcseconds—suitable for resolving compact structures in massive protostellar systems and their surrounding plasma regions [14,34].

Thanks to its flexible scheduling and high sensitivity, the system supports high-cadence monitoring—essential for detecting transient events such as accretion outbursts in high-mass protostars. These capabilities position the Irbene interferometer as a powerful tool for investigating dynamic processes in star-forming regions.

During 2020–2021, pilot observations were conducted on a small sample of methanol maser and protostellar continuum sources. These observations were used to test the full observational chain from scheduling, data acquisition, correlation, to post-processing, while also verifying system sensitivity and calibration stability. A representative example is shown in Figure 7, where small, source-intrinsic variations in both methanol maser and continuum emission in the high-mass protostar G085.410+0.003 are evident. Importantly, the stability of the gain calibration could be confirmed even without the use of standard flux calibrator sources, which were introduced later in the main program. These results demonstrated that the interferometer was operating with sufficient stability to support long-term variability studies [34].

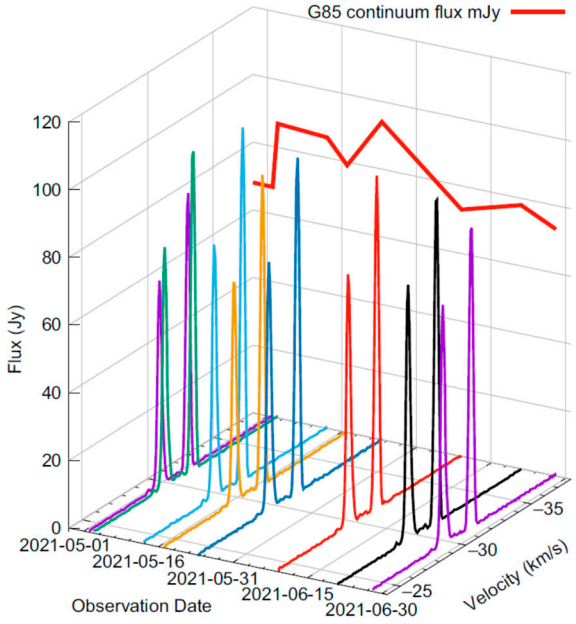

Figure 7. Methanol maser spectrum and continuum emission of the high-mass protostar G085.410+0.003, obtained during the 2020–2021 pilot observations of the IVARS project. Spectra for each epoch are coloured arbitrarily. The data illustrate intrinsic source variability and confirm the stability of the interferometer calibration [34].

In 2022, building on this interferometric infrastructure, VIRAC launched a dedicated project titled "A Single-Baseline Radio Interferometer in a New Age of Transient Astrophysics" (IVARS)[2], supported by the Latvian Science Council. The project investigates accretion-driven outbursts in high-mass star-forming regions—events triggered by the infall of material from circumstellar disks. Such events can lead to methanol maser flares and variations in continuum emission. A typical sequence involves an initial drop in continuum flux as the central object becomes obscured, followed by a rise associated with jet formation. Monitoring these changes enables the identification of burst events and the estimation of accretion timescales—key to understanding mass accumulation in young stellar objects.

A sample of 30 high-mass protostars was selected for regular monitoring. To ensure reliable bandpass and absolute flux calibration, each session began with scans of two reference maser sources (W3OH and G111.542+0.776) and two bright continuum calibrators (J2202+4216 and J2230+6946). Observations followed standard EVN practices, using a calibrator–target–calibrator cycle. Each target was observed twice per session, with integration times of 5 min for bright sources and 8 min for weaker ones; calibrators were observed in 3-min scans [14]. Observations began on 20 February 2024 and continued until 28 April 2025. During this period, a total of 236 sessions were conducted, of which 154 were successful and had their data processed for comprehensive analysis. A summary of the observed source list and the number of repetitions for each is presented in Table 1.

Table 1. Sample of 30 high-mass protostars targeted for long-term variability studies with the Irbene single-baseline interferometer.

Target Name	RA (hh:mm:ss.s)	DEC (dd:mm:ss.s)	Maser Peak Flux (Jy)	Continuum [1]	Comments	Sessions Observed
G196.45−1.68	6:14:37.69	13:49:36.2	12.2	N	periodic 110 d	18
G188.95+0.89	6:8:53.343	21:38:29.14	690	Y	periodic	14
G192.60−0.05	6:12:54.02	17:59:23.3	85	Y	past flare	15
G9.62+0.20	18:6:14.45	−20:31:27.2	5000	Y	periodic	17
G15.03−0.68	18:20:23.8	−16:11:36	13.0	Y	M17	154
G14.23−0.51	18:18:12.7	−16:49:33.8	1.2	-	-	17
G22.36+0.07	18:31:44.9	−9:22:5.01	37	N	periodic (170 d)	33
G23.71−0.20	18:35:12.07	−8:17:49.8	17.2	Y	-	33
G24.33+0.14	18:35:8.145	−7:35:1.79	5.0	N	flare recurring	33
G28.30−0.39	18:44:21.59	−4:17:33.9	15.0	Y	-	17
G29.96−0.02	18:46:3.98	−2:39:22.2	150	Y	-	17
G30.22−0.18	18:47:8.16	−2:29:42.7	16	N	-	17
G30.38−0.30	18:47:50.76	−2:24:4	8.0	N	periodic	28
G30.82−0.06	18:47:46.38	−1:54:36.7	15	N	maybe periodic	28
G31.06+0.09	18:47:41.62	−1:37:27.3	100	Y	W43	28
G33.64−0.23	18:53:32.7	0:31:50.6	120	Y	variable and periodic	15
G34.24+0.13	18:53:18.5	1:14:58.4	20	Y	-	15
G32.74−0.08	18:51:21.87	0:12:5.3	45	Y	best maser cal	15
G43.80−0.13	19:11:54.01	9:35:50.5	25	Y	periodic	14
G45.47+0.13	19:14:8.56	11:12:26.5	5	N	periodic	14
G49.60−0.25	19:23:28.93	14:40:0.8	600	N	-	14
G75.78+0.34	20:21:44.12	37:26:39.5	60	Y	-	5
G69.54−0.98	20:10:9.075	31:31:34.86	100	Y	-	5
G78.12+3.63	20:14:25.88	41:13:36.87	120	N	active maser	5
G81.77+0.60	20:39:2	42:24:59.3	2	N	-	6

Table 1. *Cont.*

Target Name	RA (hh:mm:ss.s)	DEC (dd:mm:ss.s)	Maser Peak Flux (Jy)	Continuum [1]	Comments	Sessions Observed
G81.87+0.78	20:38:36.425	42:37:34.56	500	Y	W75N	6
G85.41+0.00	20:54:13.67	44:54:8	80	Y	past flare	6
G109.87+2.11	22:56:18.12	62:1:46.3	600	Y	Cepheus A	4
G108.18+5.52	22:28:52.1	64:13:43.4	20	N	-	3
G107.30+5.64	22:21:26.81	63:51:37.14	150	-	periodic 34 d	3

[1] Detections (where '-' indicates absence) are determined based on the presence of emission of at least one contour line in the NRAO's Karl G. Jansky Very Large Array (VLA) maps [54].

In Figure 8, we present a representative example of the methanol maser and continuum flux measurements for the high-mass protostar G111.542+0.776, which is known to have a flux density of 92.8 mJy [54]. Panel (a) shows phase (top) and flux density (bottom) in the frequency domain for data generated from the coarse spectral resolution correlator pass. The maser emission is visible in "IF 3," together with the coherent phase solutions across the full observing band, demonstrating successful simultaneous detection of maser and continuum emission. Panel (b) displays the same source and data set generated with the high-resolution correlator pass, which fully resolves the methanol maser spectral profile [34]. These data, and those for the full 30 source target list, will be analysed and published in an upcoming paper. [55].

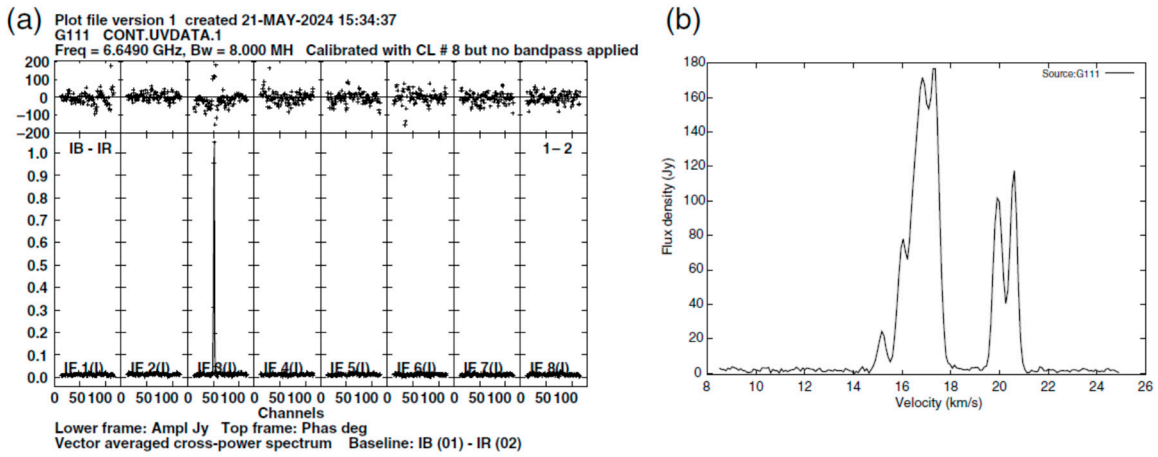

Figure 8. Simultaneous interferometric observations of the high-mass protostar G111.542+0.776. (**a**) Phase stability (top) and flux density (bottom) from the coarse spectral resolution correlator pass. Maser emission is detected in "IF 3," with coherent phase solutions across the full observing band, while spectral dilution reduces the maser amplitude. (**b**) High-resolution correlator pass of the same observation, resolving the methanol maser spectral profile [34].

The data acquisition setup employed 16 total channels (8 channels × 8 MHz per polarization) in total. Data were correlated in two stages: a continuum pass and a spectral line pass, both with 2-s integration times. The continuum data were processed using 128 FFT points, while the maser-specific channel used 4096 FFT points to achieve high spectral resolution.

Calibration was performed using a dedicated *ParselTongue* pipeline [56], which included a priori gain calibration, bandpass correction, manual phase calibration, and the application of solutions to science targets. This process delivered a spectral resolution of 0.002 MHz and a velocity resolution of 0.088 km/s. Phase and fringe-rate solutions derived from maser lines were applied to continuum data to ensure dataset alignment.

The automated and repeatable workflow provides high stability and accuracy, making the system ideally suited for tracking variability in astrophysical radio sources over extended timescales.

3.3. Observing Quasi-Periodic Pulsations in Stellar Flares with the Irbene Interferometer

Solar flares and coronal mass ejections (CMEs) represent the most energetic events within our solar system [57]. Gaining insight into the physical mechanisms that lead to these rapid and intense magnetic energy releases in the solar atmosphere remains one of the central challenges in contemporary solar physics. In recent years, increasing attention has been directed toward similar flaring phenomena occurring on other stars, especially those resembling the Sun and hosting potentially habitable exoplanets. The widely accepted "standard model" of solar flares explains the energy release through the process of magnetic reconnection [58,59].

One particularly captivating aspect of both solar and stellar flares is the occurrence of quasi-periodic pulsations (QPPs)—rhythmic modulations in flare emission that are not accounted for by the standard flare model [60–62]. QPPs have been detected across the electromagnetic spectrum, from radio waves to gamma-ray emissions, and are present in both thermal and non-thermal flare outputs. These pulsations occur in flares of all magnitudes, ranging from minor microflares [63] to the most intense flare events observed [64]. The characteristic periods of QPPs span from under a second to several minutes, or even tens of minutes in stellar superflares [58,65].

Although QPPs are frequently observed in solar flares, they are comparatively hard to detect in stellar flare data. For example, the study [58] reported a 7% detection rate of QPPs in 2274 white-light stellar flares observed with Kepler. However, the detection rate is highly sensitive to the choice of detection criteria. This relative scarcity of QPP detections enhances their scientific value. QPPs serve as effective diagnostic indicators for investigating the plasma properties and dynamic behaviour of the flare environment. Moreover, their presence indicates the incompleteness of current flare energy release models [66].

Stellar QPPs have been reported across a variety of wavelengths, including radio, X-ray, and optical (white-light) bands. Optical detections, in particular, depend heavily on high-precision photometric data from space missions such as *Kepler* and *TESS*. Interestingly, QPPs in stellar flares typically show longer periods—on the order of tens of minutes—compared to those generally seen in solar flares [67]. On the other hand, short-period QPPs have been detected in stellar flares in the radio band, e.g., [68].

One of the distinct classes of QPPs detected in both solar and stellar flares, are QPPs of the SUMER (Solar Ultraviolet Measurements of Emitted Radiation) type [69,70], which commonly appear during the flare's decay stage. These QPPs are observed as modulations in soft X-ray and extreme ultraviolet (EUV) emissions, which correspond to hot plasma activity, as well as in radio wavelengths [71]. Similar modulation patterns have been noted in the soft X-ray output of stellar flares. Notably, a linear relationship between oscillation period and damping time has been demonstrated for both solar and stellar QPPs of the SUMER type [67]. Furthermore, analogous QPP signatures have been detected in the white-light emissions of stellar flares [65,72], reinforcing the notion of fundamental physical parallels between solar and stellar flare processes [57].

In 2023, VIRAC launched the Latvian Science Council-funded project "Multi-Wavelength Study of Quasi-Periodic Pulsations in Solar and Stellar Flares (STEF)"[3]. One of the objectives of the project is to investigate QPPs in the radio domain. To support this, a dedicated single-baseline radio interferometer operating in the 4.5–8.8 GHz frequency range is employed. The system is optimized for one-second time resolution—crucial for capturing the short-period oscillations that characterize QPPs. Unlike conventional large-array inter-

ferometers designed primarily for high spatial resolution, this setup is purpose-built for time-domain astrophysics. Its focus is on detecting variability and analyzing the temporal structure of flaring events, providing a unique toolset for investigating the underlying mechanisms of stellar flares in nearby active stars.

The data-processing pipelines use *SFXC* correlation, *AIPS*, and *ParselTongue* scripting—which were originally developed and optimized for Galactic maser observations as part of the *IVARS* project. In the *STEF* project, these existing pipelines have been utilized for the analysis of continuum flux associated with stellar flare variability, without requiring significant modification.

Signal cross-correlation between the two antennas significantly increases the signal-to-noise ratio compared to single-dish systems, enabling enhanced sensitivity and reducing radio frequency interference (RFI). This configuration—rare in today's research environment dominated by shared, multi-user large arrays—offers flexible, autonomous operation, allowing for targeted and regular monitoring of stellar flare activity at the cadence required for QPP detection.

Since November 2023, VIRAC has carried out nine observational campaigns focused on active M-dwarf stars such as *EV Lac* and *AD Leo*, which are recognized for their high flare frequency and energetic outbursts (see Table 2 for campaign details). These characteristics make them ideal candidates for investigating stellar flare dynamics and the occurrence of quasi-periodic pulsations (QPPs). These stars were selected based on radio brightness, flare occurrence rates, and favourable sky positions. Observations are conducted in dual polarization, providing sensitivity to both total intensity and magnetic field variations. The current observational strategy prioritizes high cadence (i.e., second-scale resolution), essential for resolving QPPs with periods as short as a few seconds.

Table 2. Single dish and single-baseline interferometric observation of stellar flares.

Date & Time, UTC	Experiment Code	Sources	Antennas	Frequences, Channel Number Channel Bandwidth
5 April 2024, 11:25–15:20	stef4k	AD Leonis (Gliese 388), EV Lacertae (Gliese 873), 2050 + 364, J1959+4044	RT-32 & RT-16	6659.69 MHz; 16; 16 MHz
22 March 2024,11:15–16:15	stef1k, stef3k	AD Leonis (Gliese 388), EV Lacertae (Gliese 873), 2050 + 364	RT-32 & RT-16	6659.82 MHz; 16; 16 MHz
3 February 2024,11:00–13:00	stefk2	EV Lacertae (Gliese 873), G75, Cygnus X-1, 3C 345	RT-32	6656.39 MHz; 16; 8 MHz
25 January 2024,15:45–02:00	stefk1	EV Lacertae (Gliese 873), 3C 196, 3C 196+, DA 193, DA193+, 3C 138, 3C138+	RT-32	6656.36 MHz; 16; 8 MHz
18 December 2023, 15:45–02:20	stef24	EV Lacertae (Gliese 873), 3C 454.3	RT-32	6656.31 MHz; 16; 8 MHz
8 December 2023,18:00–23:59	stef23	EV Lacertae (Gliese 873)	RT-32	6656.33 MHz; 16; 8 MHz
8 December 2023,16:45–17:05	too1	W3(OH), Omega Nebula (M17), 3C 345, J2230+6946	RT-32 & RT-16	8003.6 MHz; 16; 8 MHz
1 December 2023,18:00–24:00	stef22	EV Lacertae (Gliese 873)	RT-32	6656.35 MHz; 16; 8 MHz
24 November 2023,17:00–02:00	stef21	EV Lacertae (Gliese 873)	RT-32	6656.38 MHz; 16; 8 MHz

Preliminary results affirm the importance of using an interferometric system for the detection of stellar flare signatures. Single-dish observations with the RT-32 telescope alone proved insufficiently sensitive to detect flare-associated continuum variability. Although no clear flares were identified in the initial datasets, modelling indicates that the interferometer

is capable of detecting low-amplitude flux variations on the order of tens of millijanskys—comparable to the expected signatures of quasi-periodic pulsations (QPPs). These findings underscore the capability of the Irbene interferometric system for high-precision monitoring of transient stellar radio emissions.

The next phase of the project, scheduled from autumn 2025 to spring 2026, will broaden the observational scope through a sustained monitoring campaign aimed at capturing a statistically meaningful sample of QPP events in stellar flares. These observations will be complemented by simultaneous optical monitoring in collaboration with partner institutions, enabling multi-wavelength correlation studies. By integrating radio and optical diagnostics, the project seeks to better constrain the physical mechanisms responsible for QPPs and advance our understanding of flare dynamics in stellar coronae. Beyond stellar applications, radio observations such as these also hold promise for solar flare forecasting. As shown in recent work [73], radio monitoring of active regions in the microwave range can serve as an early warning tool for solar flares, offering a valuable extension to the capabilities developed within the STEF project.

3.4. Future Developments—Custom Correlator and Advanced Data Processing Frameworks for VLBI Science

Recent advances in computing hardware and software frameworks have opened new opportunities for enhancing VLBI performance, particularly in compact interferometric systems. One of the most promising developments has been the widespread availability of GPUs featuring specialized cores for Artificial intelligence (AI) and matrix operations. For instance, NVIDIA's introduction of *Tensor Cores* in 2017 has substantially accelerated high-throughput matrix multiplication tasks—a key operation in radio interferometric correlation—by exploiting low-precision arithmetic units optimized for parallelism [74]. Leveraging such hardware architectures offers a clear pathway to reducing computational bottlenecks in VLBI correlators.

In parallel, modern data processing frameworks such as *Dask*[4] have matured, enabling scalable, distributed handling of large datasets across heterogeneous computing environments. *Dask* is particularly well suited to radio astronomy pipelines due to its support for parallel array processing and dynamic task scheduling.

To capitalize on these technological advancements for VLBI science, the RADIOBLOCKS consortium[5] was established, bringing together research institutions and infrastructure operators to develop next-generation software correlators and data processing platforms. Within this framework, the VIRAC team is contributing to the development of a new GPU-accelerated correlator specifically optimized for the scientific goals of the Irbene Single-Baseline Interferometer. The design builds upon the architecture and lessons learned from the AARTFAAC (*Amsterdam-ASTRON Radio Transients Facility and Analysis Center*) correlator [75], which demonstrated the feasibility of using high-performance, low-latency hardware for transient radio signal detection.

The ISBI-dedicated correlator under development we expect to be tailored for high time-resolution, broadband observations across the L, C and X bands, aligning with the existing capabilities of the RT-32 and RT-16 telescopes. In addition to standard correlation outputs, the system will support near real-time fringe fitting and beamforming modes, facilitating rapid data assessment and enabling adaptive observation strategies.

Alongside correlator development, the VIRAC team is also constructing a modular, scalable data processing pipeline based on the *Dask* framework. This pipeline will handle tasks ranging from calibration and RFI mitigation to spectral line extraction and time-series analysis. Special emphasis is placed on the incorporation of advanced signal decomposition techniques such as Singular Spectrum Analysis (SSA) for robust identification and removal of RFI, particularly in dynamic spectral environments.

The combined deployment of a dedicated, GPU-enabled correlator and a flexible Dask-based processing pipeline represents a significant step forward in enhancing the autonomy, throughput, and scientific reach of the Irbene interferometric system. These developments position ISBI as a modern, agile instrument capable of contributing to both time-domain astrophysics and space weather diagnostics in the evolving landscape of radio astronomy.

4. Discussion and Conclusions

The Irbene single-baseline radio interferometer—comprising the 32-m RT-32 and the 16-m RT-16 antennas—constitutes a unique and strategically important asset in contemporary radio astronomy. Although it does not offer the ultra-high spatial resolution of large VLBI arrays, its compact 800-m baseline, combined with its high sensitivity, makes it exceptionally well-suited for time-domain studies and signal-sensitive applications. This paper has outlined the system's technical architecture and explored its broad scientific utility, demonstrating its effectiveness across multiple research domains. The highlighted use cases span both practical applications and fundamental research, underscoring the interferometer's versatility and value to the scientific community.

One key area of application is ionospheric remote sensing and GNSS orbit determination using L-band interferometry. VLBI observations of navigation satellite signals—conducted in collaboration with international partners and Satellite Laser Ranging (SLR) stations—enable precise ionospheric diagnostics and support the development of hybrid satellite orbit solutions.

Another important use of the system lies in Forward Scatter Radar (FSR) techniques for detecting satellites, space debris, and aircraft. By employing GNSS signals and natural radio sources as illumination, the Irbene interferometer has successfully demonstrated the forward scatter effect in a bistatic configuration, laying the groundwork for future contributions to space situational awareness.

In the field of astrophysics, the system supports the monitoring of the 6.7 GHz methanol maser and radio continuum variability in the high-mass star-forming regions. Its high-cadence and broadband observing capabilities enable long-term studies of variability, revealing periodic and episodic flux changes that reflect the dynamic environments of massive protostars. While maser and continuum emissions—both thermal (from O/B-type stars) and non-thermal (arising from ionized outflows and jet-driven shocks)—are of key interest, the 32 m antenna alone lacks the resolution and sensitivity with which to independently detect and distinguish these components. Moreover, interferometric arrays such as the EVN tend to resolve out extended emission, underscoring the need for a complementary system capable of bridging the gap between single-dish sensitivity and VLBI resolution.

The ISBI is expected to help address these challenges and enable the detection of quasi-periodic pulsations (QPPs) in stellar flares, potentially contributing to a deeper understanding of magnetohydrodynamic processes in active stars. Its planned temporal resolution and sensitivity are designed to make it well-suited for capturing short-lived phenomena such as QPPs and flux oscillations during flaring events.

Collectively, these applications highlight the strategic relevance of compact interferometric systems in an era increasingly dominated by large-scale observatories. The Irbene interferometer offers flexible access to high-sensitivity observations, rapid reconfigurability, and dedicated observation time—qualities that are essential for sustained monitoring, experimental campaigns, and multi-instrument coordination. Future developments, including integration with the EVN-Lite network, collaboration with other European antennas operating in similar wavelength ranges, and the anticipated expansion of receiver capabili-

ties, show promise with respect to further enhancing the scientific potential of the Irbene facility across the domains of radio astronomy, space geodesy, and space weather research.

Author Contributions: Conceptualization, I.S., V.B., J.Š., K.Š., A.A., R.A.B., D.Y.K., V.M.N. and S.A.B.; methodology, I.S., V.B., J.Š., K.Š., A.A., R.A.B., D.Y.K. and D.B.; software, I.S., V.B., J.Š., K.Š., A.A., R.A.B., M.P. and M.B.; validation, V.B., J.Š., K.Š., A.A. and R.A.B.; formal analysis, V.B., J.Š., K.Š., A.A., R.A.B., A.K. and S.A.B.; investigation, V.B., J.Š., K.Š., A.A., R.A.B. and A.K.; resources, V.B., J.Š., K.Š., A.A., R.A.B., A.K. and A.O.; data curation, V.B., J.Š., K.Š., A.A., R.A.B., A.K. and A.O.; writing—original draft preparation, I.S. and V.B.; writing—review and editing, I.S., V.B., J.Š., A.A., R.A.B., V.M.N. and M.K.; visualization, V.B.; supervision, I.S., V.B., J.Š., K.Š., R.A.B., D.Y.K. and V.M.N.; project administration, I.S., V.B., K.Š., R.A.B., D.Y.K. and V.M.N.; funding acquisition, I.S., V.B., J.Š., K.Š., A.A., R.A.B., D.Y.K. and V.M.N. All authors have read and agreed to the published version of the manuscript.

Funding: This research was funded by Latvian Council of Science, Fundamental and Applied Research Project "A single-baseline radio interferometer in a new age of transient astrophysics (IVARS)", grant number lzp-2022/1-0083.

Data Availability Statement: Data are contained within the article.

Acknowledgments: During the preparation of this manuscript, the authors used ChatGPT-4.5, based on the GPT-4.5 architecture, to assist with English grammar and stylistic improvements. All outputs were reviewed and edited by the authors, who take full responsibility for the final content of this publication.

Conflicts of Interest: The authors declare no conflicts of interest.

Abbreviations

The following abbreviations are used in this manuscript:

AARTFAAC	Amsterdam-ASTRON Radio Transients Facility and Analysis Center
ALMA	the Atacama Large Millimetre/submillimetre Array
AI	Artificial intelligence
AIPS	Astronomical Image Processing System
ASKAP	the Australian Square Kilometre Array Pathfinder
CASA	Common Astronomy Software Applications
CMEs	Coronal Mass Ejections
DBBC	Digital Baseband Converter
EHT	the Event Horizon Telescope
GLONASS	a Russian satellite navigation system
GNSS	Global Navigation Satellite System
GPS	Global Positioning System
EVN	as the European VLBI Network
FAST	the Five-hundred-meter Aperture Spherical Telescope, China
FRB	Fast Radio Burst FRB
FSR	Forward Scatter Radar
ISBI	Irbene Single Baseline Radio Interferometer
JIVE	the Joint Institute for VLBI in Europe ERIC
LOFAR	Low-Frequency Array
LNA	Low-Noise Amplifier
LCP and RCP	Left and Right Circular Polarization
MeerKAT	Meer Karoo Array Telescope is a radio interferometer located in the Karoo region of South Africa
NEO	Near-Earth Object (Orbit)
NRAO	The U.S. National Science Foundation National Radio Astronomy Observatory
OMT	Orthomode Transducer

RFI	Radio Frequency Interference
SEFD	System Equivalent Flux Density
SFXC	the Software FX Correlator
SLR	Satellite Laser Ranging
SUMER	Solar Ultraviolet Measurements of Emitted Radiation
QPP	Quasi-Periodic Pulsations
VIRAC	Ventspils International Radio Astronomy Centre
VDIF	VLBI Data Interchange Format
VLBI	Very Long Baseline Interferometry
VLA	the NRAO's Karl G. Jansky Very Large Array
VUAS	Ventspils University of Applied Sciences
WSRT	the Westerbork Syn-thesis Radio Telescope

Notes

[1] Upgraded SURA (http://eng.unn.ru/news/upgraded-sura-facility-launched, accessed on 15 October 2025) facility, the Univer-sity of Nizhni Novgorod.

[2] Latvian Council of Science, Fundamental and Applied Research Project "A single-baseline radio interferometer in a new age of transient astrophysics (IVARS (https://en.venta.lv/zinatne/projekti/a-single-baseline-radio-interferometer-in-a-new-age-of-transient-astrophysics, accessed on 15 October 2025))". No.: lzp-2022/1-0083. Duration: 1 January 2023–31 December 2025. Budget 300 kEuro.

[3] Latvian Council of Science, Fundamental and Applied Research Project "Multi-Wavelength Study of Quasi-Periodic Pulsa-tions in Solar and Stellar Flares (STEF (https://en.venta.lv/zinatne/projekti/multi-wavelength-study-of-quasi-periodic-pulsations-in-solar-and-stellar-flares, accessed on 15 October 2025))". No.: lzp-2022/1-0017. Duration: 1 January 2023–31 December 2025. Budget 300 kEuro.

[4] Dask (https://www.dask.org/, accessed on 15 October 2025)—flexible parallel computing library for Python 3.14 that enables scalable data analysis and numerical computation across multiple cores, machines, or clusters.

[5] EU Horizon Europe research and innovation project "New science in Radio Astronomy: applying cutting-edge technology to enhance the entire data chain, from receiver to final output (RADIOBLOCKS (https://radioblocks.eu/, accessed on 15 October 2025))". No 101093934. Duration 1 March 2023–28 February 2027. Budget 8.9 MEur.

References

1. Ryle, M.; Vonberg, D.D. Solar radiation on 175 Mc./s. *Nature* **1946**, *158*, 339. Available online: https://ui.adsabs.harvard.edu/link_gateway/1946Natur.158..339 (accessed on 15 October 2025). [CrossRef]
2. Venturi, T.; Paragi, Z.; Lindqvist, M.; Bartkiewicz, A.; Beswick, R.; Bogdanović, T.; Brisken, W.; Charlot, P.; Colomer, F.; Conway, J.; et al. VLBI20-30: A Scientific Roadmap for the Next Decade—The Future of the European VLBI Network. *arXiv* **2020**, arXiv:2007.02347.
3. Preuss, E. Very Long Baseline Interferometry (VLBI) from ground and space. *ESA Space Sci. Fundam. Phys.* **1988**, *283*, 105–116. Available online: https://adsabs.harvard.edu/full/1988ESASP.283..105P (accessed on 15 October 2025).
4. Wootten, A.; Thompson, A.R.; ALMA Development Roadmap Committee. *The Atacama Large Millimeter/Submillimeter Array (ALMA): A White Paper Submitted to the Astro2010 Decadal Survey Committee*; NRAO: Charlottesville, VA, USA, 2009. Available online: https://www.nrao.edu/A2010/rfi/ALMA-edited.pdf (accessed on 15 October 2025).
5. Event Horizon Telescope Collaboration. First M87 Event Horizon Telescope Results. I. The Shadow of the Supermassive Black Hole. *Astrophys. J. Lett.* **2019**, *875*, L1. [CrossRef]
6. Event Horizon Telescope Collaboration. First Sagittarius A* Event Horizon Telescope Results. I. The Shadow of the Supermassive Black Hole in the Galactic Center. *Astrophys. J. Lett.* **2022**, *930*, L12. [CrossRef]
7. Johnson, M.D.; Akiyama, K.; Blackburn, L.; Bouman, K.L.; Broderick, A.E.; Cardoso, V.; Fender, R.P.; Fromm, C.M.; Galison, P.; Gómez, J.L.; et al. Key Science Goals for the Next-Generation Event Horizon Telescope. *Galaxies* **2023**, *11*, 61. [CrossRef]
8. Goedhart, S.; Magnus, L. MeerKAT Science Operations and Lessons Learned. *Proc. SPIE* **2024**, *13098*, 130980X. [CrossRef]
9. Shannon, R.M.; Bannister, K.W.; Bera, A.; Bhandari, S.; Day, C.K.; Deller, A.T.; Dial, T.; Dobie, D.; Ekers, R.D.; Fong, W.-F.; et al. The Commensal Real-Time ASKAP Fast Transient Incoherent-Sum Survey. *Publ. Astron. Soc. Aust.* **2025**, *42*, e036. [CrossRef]
10. Effelsberg 100-m Radio Telescope. Max-Planck-Institut für Radioastronomie. Available online: https://www.mpifr-bonn.mpg.de/effelsberg (accessed on 15 October 2025).
11. FAST Collaboration; Jiang, P.; Yue, Y.; Gan, H.; Yao, R.; Li, H.; Pan, G.; Sun, J.; Yu, D.; Liu, H.; et al. Commissioning progress of the FAST, Science China Physics. *Mech. Astron.* **2019**, *62*, 959502. [CrossRef]

12. Braatz, J.A.; Reid, M.J.; Henkel, C. The Megamaser Cosmology Project. *Astrophys. J.* **2010**, *718*, 657–665. [CrossRef]
13. Ozeki, M.; Heki, K. Recent Results of the GNSS Total Electron Content Measurements and Their Implications for Ionospheric Disturbances. *AGU Fall Meet. Abstr.* **2022**. SA53A-01. Available online: https://ui.adsabs.harvard.edu/abs/2022AGUFMSA53A..01O/abstract (accessed on 15 October 2025).
14. Šteinbergs, J.; Škirmante, K.; Aberfelds, A.; Bezrukovs, V.; Shmeld, I.; Burns, R.A. Interferometer for variable astrophysical radio sources. *J. Astron. Telesc. Instrum. Syst.* **2025**, *11*, 018001. [CrossRef]
15. Hogbom, J.A.; Brouw, W.N. The Synthesis Radio Telescope at Westerbork. Principles of Operation, Performance and Data Reduction. *Astron. Astrophys.* **1974**, *33*, 289. Available online: https://ui.adsabs.harvard.edu/abs/1974A%26A....33..289H/abstract (accessed on 15 October 2025).
16. Perley, R.A.; Chandler, C.J.; Butler, B.J.; Wrobel, J.M. The Expanded Very Large Array: A New Telescope for New Science. *Astrophys. J. Lett.* **2011**, *739*, L1. [CrossRef]
17. Thompson, A.R.; Moran, J.M.; Swenson, G.W. *Interferometry and Synthesis in Radio Astronomy*, 3rd ed.; Springer: Berlin/Heidelberg, Germany, 2017. Available online: https://link.springer.com/book/10.1007/978-3-319-44431-4 (accessed on 15 October 2025).
18. Kurtz, S. Hypercompact HII regions. *Massive Star Birth A Crossroads Astrophys.* **2005**, *227*, 111–119. [CrossRef]
19. Dewdney, P.; Braun Turner, R.W.; Santander-Vela, J.; Waterson, M.; Tan, G. SKA1 System Baseline Design, Version 2.1. In *SKA Organisation Technical Report SKA-TEL-SKO-0000002-Rev03*; SKA Organisation: Macclesfield, UK, 2016. Available online: https://www.skao.int/sites/default/files/documents/d1-SKA-TEL-SKO-0000002_03_SKA1SystemBaselineDesignV2_1.pdf (accessed on 15 October 2025).
20. Murphy, E.J.; Bolatto, A.; Chatterjee, S.; Casey, C.M.; Chomiuk, L.; Dale, D.; de Pater, I.; Dickinson, M.; Di Francesco, J.; Hallinan, G.; et al. Science with an ngVLA: The ngVLA Science Case and Associated Science Requirements. *arXiv* **2018**. [CrossRef]
21. Bezrukovs, V.; Shmeld, I. First successful VLBI observations in the EVN with VIRAC radio telescope RT-32. In Proceedings of the 11th European VLBI Network Symposium & Users Meeting, Bordeaux, France, 9–12 October 2012; p. 78. [CrossRef]
22. Skirmante, K.; Bezrukovs, V.; Jekabsons, N.; Shmeld, I. Preparation of the VIRAC Radio Telescope RT-32 for E-VLBI Observations. *Balt. Astron.* **2013**, *22*, 329–340. [CrossRef]
23. Bezrukovs, V. First interferometric observations in Irbene—Torun baseline conducted by VIRAC. In Proceedings of the 14th European VLBI Network Symposium & Users Meeting (EVN 2018), Granada, Spain, 8–11 October 2018; p. 131. [CrossRef]
24. Hewitt, D.M. A Repeating Fast Radio Burst Source in a Low-luminosity Dwarf Galaxy. *Astrophys. J.* **2024**, *977*, L4. [CrossRef]
25. Hewitt, D.M. Milliarcsecond localization of the hyperactive repeating FRB 20220912A. *Mon. Not. R. Astron. Soc.* **2024**, *529*, 1814–1826. [CrossRef]
26. Nechaeva, M.; Antipenko, A.; Bezrukovs, D.; Bezrukov, D.; Dementjev, A.; Dugin, N.; Konovalenko, A.; Kulishenko, V.; Liu, X.; Nabatov, A.; et al. A experiment on radio location of objects in the near-Earth space with VLBI in 2012. *Balt. Astron.* **2013**, *22*, 35–41. [CrossRef]
27. Kovalev, Y.; Kardashev, N.; Sokolovsky, K.; Voitsik, P.; An, T.; Anderson, J.; Andrianov, A.; Avdeev, V.; Bartel, N.; Bignall, H.; et al. Detection statistics of the RadioAstron AGN survey. *Adv. Space Res.* **2020**, *65*, 705–711. [CrossRef]
28. Tuccari, G.; Bezrukovs, V.; Nechaeva, M. Digital Base Band Converter As Radar VLBI Backend. *Latv. J. Phys. Tech. Sci.* **2012**, *49*, 18–29. [CrossRef]
29. Bleiders, M. Spectral Line Registration Backend Based on USRP X300 Software Defined Radio. *J. Astron. Instrum.* **2020**, *9*, 2050009. [CrossRef]
30. Bezrukovs, V. Receiving And Data Acquisition Systems Of RT-32 For VLBI Observations. *Latv. J. Phys. Tech. Sci.* **2012**, *49*, 30–42. [CrossRef]
31. Bezrukovs, V. Time and Frequency Synchronization on the Virac Radio Telescope RT-32. *Latv. J. Phys. Tech. Sci.* **2016**, *53*, 14–19. [CrossRef]
32. Hendre, A.; Alachkar, B.; Boven, P.; Chen, S.; Collingwood, H.; Davis, J.; Dewdney, P.; Gozzard, D.; Grainge, K.; Gravestock, C.; et al. Precise Timescale, Frequency, and Time-Transfer Technology for the Square Kilometer Array. *J. Astron. Telesc. Instrum. Syst.* **2022**, *8*, 011022. [CrossRef]
33. Keimpema, A.; Kettenis, M.M.; Pogrebenko, S.V.; Campbell, R.M.; Cimó, G.; Duev, D.A.; Eldering, B.; Kruithof, N.; van Langevelde, H.J.; Marchal, D.; et al. The SFXC Software Correlator for Very Long Baseline Interferometry: Algorithms and Implementation. *Exp. Astron* **2015**, *39*, 259–279. Available online: https://link.springer.com/article/10.1007/s10686-015-9446-1 (accessed on 15 October 2025). [CrossRef]
34. Steinbergs, J. Single-baseline interferometer for mJy observations. In Proceedings of the European VLBI Network Mini-Symposium and Users' Meeting 2021, Online, 12–14 July 2021; Volume 2021, p. 33. [CrossRef]
35. Bezrukovs, V.; Bleiders, M.; Orbidans, A.; Bezrukovs, D. Broadband receiving systems for 4.58-8.8 GHz radio astronomical observations at Irbene radio telescopes RT-32 and RT-16. *arXiv* **2020**. [CrossRef]
36. Antyufeyev, O. Receiver gain and system temperature instability during the calibration of spectral data at radio telescopes in C-band. *Astron. Astrophys. Trans.* **2022**, *33*, 113–122. [CrossRef]

37. Antyufeyev, O.; Bleiders, M.; Patoka, O.; Bezrukovs, V.; Shmeld, I.; Shulga, V. Atmospheric opacity correction in C-band at Irbene RT-16 radio telescope. *Astron. Astrophys. Trans.* **2022**, *33*, 103–112. [CrossRef]
38. Antyufeyev, O. Estimation of errors at the calibration of spectral data at the Irbene RT-32 radio telescope. *Astron. Astrophys. Trans.* **2020**, *32*, 23–38. [CrossRef]
39. Bleiders, M.; Bezrukovs, V.; Orbidans, A. Performance Evaluation of Irbene RT-16 Radio Telescope Receiving System. *Latv. J. Phys. Tech. Sci.* **2017**, *54*, 42–53. [CrossRef]
40. Trokss, J.; Lesins, A.; Gaigals, G.; Nechaeva, M.; Bezrukovs, V. Receiving System For Ionosphere Research. *Latv. J. Phys. Tech. Sci.* **2012**, *49*, 13–17. [CrossRef]
41. Bleiders, M.; Berzins, A.; Jekabsons, N.; Skirmante, K.; Bezrukovs, V. Low-Cost L-Band Receiving System Front-End for Irbene RT-32 Cassegrain Radio Telescope. *Latv. J. Phys. Tech. Sci.* **2019**, *56*, 50–61. [CrossRef]
42. Skirmante, K.; Bezrukovs, V.; Bleiders, M.; Jasmonts, G.; Jekabsons, N.; Nechaeva, M. Observations of Weak Galactic OH Masers in 1.6 GHz Frequency Band Using Irbene RT-32 Radio Telescope. *Latv. J. Phys. Tech. Sci.* **2022**, *59*, 14–22. [CrossRef]
43. Dugin, N.; Antipenko, A.; Bezrukovs, V.; Gavrilenko, V.; Dementjev, A.; Lesins, A.; Nechaeva, M.; Shmeld, I.; Snegirev, S.; Tikhomirov, Y.; et al. Radio interferometric research of ionosphere by signals of space satellites. *Balt. Astron.* **2013**, *22*, 25–33. [CrossRef]
44. Nechaeva, M.; Adamchik, D.; Bezrukovs, V.; Dugin, N.; Shmeld, I.; Tikhomirov, Y. Measurements of Interferometer Parameters at Reception of GLONASS and GPS Signals. *Latv. J. Phys. Tech. Sci.* **2016**, *53*, 24–30. [CrossRef]
45. Skirmante, K.; Jekabsons, N.; Graps, A.; Bezrukovs, V.; Bleiders, M.; Nachaeva, M. Near Earth Objects: Observations with VIRAC Radiotelescopes in VLBI Mode. *Eur. Planet. Sci. Congr.* **2017**, *11*, EPSC2017-867. Available online: https://ui.adsabs.harvard.edu/abs/2017EPSC...11..867S (accessed on 15 October 2025).
46. Skirmante, K.; Jekabsons, N.; Salmins, K.; Bezrukovs, V.; Nechaeva, M. The Joint SLR (Optical Range) and Radar-VLBI Satellite Observations using VIRAC Radio Telescope RT32, RT16 and SLR Station Riga. *Latv. J. Phys. Tech. Sci.* **2020**, *57*, 62–70. [CrossRef]
47. Kotlere, D.; Jekabsons, N.; Nechaeva, M.; Smelds, I. Algorithmic Development of Software Correlator for Space Debris Data Processing in VIRAC. *VIRAC Space Res. Rev.* **2012**, *1*, 57–67. Available online: https://irp-cdn.multiscreensite.com/0502f3c5/files/uploaded/Space-228lpp-175x250_2012.pdf (accessed on 15 October 2025).
48. Skirmante, K. Observations of astronomical objects using radio (Irbene RT-32 telescope) and optical (Baldone Schmidt) methods. *Astron. Astrophys. Trans.* **2020**, *32*, 13–22. [CrossRef]
49. Bezrukovs, V.; Dugin, N.; Skirmante, K.; Jasmons, G.; Šteinbergs, J. The forward scatter radar method for detecting space objects using emission of extraterrestrial radio sources. In Proceedings of the 2nd NEO and Debris Detection Conference, Darmstadt, Germany, 24–26 January 2023; p. 94. Available online: https://ui.adsabs.harvard.edu/abs/2023sndd.confE..94B (accessed on 15 October 2025).
50. Shmeld, I.; Aberfelds, A.; Bērziņš, K.; Bezrukovs, V.; Bleiders, M.; Orbidans, A. First Galactic Maser Observations on Ventspils Radio Telescopes—Instrumentation and Data Reduction. *Astrophys. Masers Unlocking Myster. Universe* **2018**, *336*, 445–446. [CrossRef]
51. Patoka, O. New ex-OH maser detections in the northern celestial hemisphere. *Astron. Astrophys.* **2021**, *652*, A17. [CrossRef]
52. Aberfelds, A. 6.7 GHz Methanol Masers Studies: Observation Methods, Monitoring and Morphology of Sources. Ph.D. Thesis, University of Latvia, Rīga, Latvia, 2024. Available online: https://ui.adsabs.harvard.edu/abs/2024PhDT.....1A (accessed on 15 October 2025).
53. Aberfelds, A.; Šteinbergs, J.; Shmeld, I.; Burns, R.A. Five years of 6.7-GHz methanol maser monitoring with Irbene radio telescopes. *Mon. Not. R. Astron. Soc.* **2023**, *526*, 5699–5714. [CrossRef]
54. Hu, B.; Wang, J.; Henkel, C.; Menten, K.M.; Xu, Y. On the relationship of UC H II regions and class II methanol masers. I. Source catalogs. *Astrophys. J.* **2016**, *833*, 1. [CrossRef]
55. Burns, R.A.; Šteinbergs, J.; Šķirmante, K.; Bezrukovs, V.; Aberfelds, A.; Shmeld, I.; Campbell, B.; Verkouter, M.; Keimpema, A. RIKEN Pioneering Research Institute, 2-1 Hirosawa, Wako-shi, 351-0198, Saitama, Japan. 2025; *manuscript in preparation*.
56. Kettenis, M.; van Langevelde, H.J.; Reynolds, C.; Cotton, B. ParselTongue: AIPS Talking Python. *Astron. Data Anal. Softw. Syst. XV* **2006**, *351*, 497. Available online: https://aspbooks.org/custom/publications/paper/351-0497.html (accessed on 15 October 2025).
57. Benz, A.O. Flare Observations. *Living Rev. Sol. Phys.* **2017**, *14*, 2. Available online: https://link.springer.com/article/10.1007/s41116-016-0004-3 (accessed on 15 October 2025). [CrossRef]
58. Belov, S.A.; Kolotkov, D.Y.; Nakariakov, V.M.; Broomhall, A.-M. Detecting Quasiperiodic Pulsations in Solar and Stellar Flares with a Neural Network. *Astrophys. J. Suppl. Ser.* **2024**, *274*, 31. [CrossRef]
59. Shibata, K.; Magara, T. Solar Flares: Magnetohydrodynamic Processes. *Living Rev. Sol. Phys.* **2011**, *8*, 6. [CrossRef]
60. Nakariakov, V.M.; Melnikov, V.F. Quasi-Periodic Pulsations in Solar Flares. *Space Sci. Rev.* **2009**, *149*, 119. [CrossRef]
61. Nakariakov, V.M.; Inglis, A.R.; Zimovets, I.V.; Foullon, C.; Verwichte, E.; Sych, R.; Myagkova, I.N. Oscillatory processes in solar flares. *Plasma Phys. Control. Fusion* **2010**, *52*, 124009. [CrossRef]

62. Zimovets, I.V.; McLaughlin, J.A.; Srivastava, A.K.; Kolotkov, D.Y.; Kuznetsov, A.A.; Kupriyanova, E.G.; Cho, I.-H.; Inglis, A.R.; Reale, F.; Pascoe, D.J.; et al. Quasi-Periodic Pulsations in Solar and Stellar Flares: A Review of Underpinning Physical Mechanisms and Their Predicted Observational Signatures. *Space Sci. Rev.* **2021**, *217*, 66. [CrossRef]
63. Nakariakov, V.M.; Anfinogentov, S.; Storozhenko, A.A.; Kurochkin, E.A.; Bogod, V.M.; Sharykin, I.N.; Kaltman, T.I. Quasi-periodic Pulsations in a Solar Microflare. *Astrophys. J.* **2018**, *859*, 154. [CrossRef]
64. Kolotkov, D.Y.; Pugh, C.E.; Broomhall, A.-M.; Nakariakov, V.M. Quasi-periodic Pulsations in the Most Powerful Solar Flare of Cycle 24. *Astrophys. J. Lett.* **2018**, *858*, L3. [CrossRef]
65. Pugh, C.E.; Armstrong, D.J.; Nakariakov, V.M.; Broomhall, A.-M. Statistical properties of quasi-periodic pulsations in white-light flares observed with Kepler. *Mon. Not. R. Astron. Soc.* **2016**, *459*, 3659–3676. [CrossRef]
66. Panferov, A.; Kolotkov, D.; Beskin, G.; Karpov, S.; Plokhotnichenko, V.; Maryeva, O. Quasi-periodic pulsations in flares of UV Ceti-type stars. *Mod. Astron. Early Universe Exopl. Black Holes (VAK2024)* **2024**, *1*, 496–500. [CrossRef]
67. Cho, I.H.; Cho, K.S.; Nakariakov, V.M.; Kim, S.; Kumar, P. Comparison of damped oscillations in solar and stellar x-ray flares. *Astrophys. J.* **2016**, *830*, 110. [CrossRef]
68. Zaitsev, V.V.; Kislyakov, A.G.; Stepanov, A.V.; Kliem, B.; Furst, E. Pulsating Microwave Emission from the Star AD Leo. *Astron. Lett.* **2004**, *30*, 319–324. Available online: https://link.springer.com/article/10.1134/1.1738154 (accessed on 15 October 2025). [CrossRef]
69. Wang, T. Standing Slow-Mode Waves in Hot Coronal Loops: Observations, Modeling, and Coronal Seismology. *Space Sci. Rev.* **2011**, *158*, 397. [CrossRef]
70. Wang, T.; Ofman, L.; Yuan, D.; Reale, F.; Kolotkov, D.Y.; Srivastava, A.K. Slow-Mode Magnetoacoustic Waves in Coronal Loops. *Space Sci. Rev.* **2021**, *217*, 34. [CrossRef]
71. Kim, S.; Nakariakov, V.M.; Shibasaki, K. Kink Oscillations of Coronal Loops. *Astrophys. J. Lett.* **2012**, *756*, L36. [CrossRef]
72. Bai, J.-Y.; Wang, J.; Li, H.L.; Xin, L.P.; Li, G.W.; Yang, Y.G.; Wei, J.Y. Photometric Observations of Flares on AD Leo from GWAC-F30 and TESS. *Publ. Astron. Soc. Pac.* **2023**, *135*, 064201. [CrossRef]
73. Popova, E.; Bezrukovs, D.; Bezrukovs, V.; Suchikova, Y.; Popov, A.I. Radio-astronomical monitoring of active regions in the microwave range in the service of forecasting solar flares. *Mod. Phys. Lett. A* **2024**, *39*, 2450069. [CrossRef]
74. Romein, J.W. The Tensor-Core Correlator. *Astron. Astrophys.* **2021**, *656*, A52. [CrossRef]
75. Prasad, P.; Wijnholds, S.J.; Huizinga, F.; Wijers, R.A.M.J. Real-time calibration of the AARTFAAC array for transient detection. *Astron. Astrophys.* **2014**, *568*, A48. [CrossRef]